BBA - General Subjects 1864 (2020) 129531

Contents lists available at ScienceDirect

BBA - General Subjects

journal homepage: www.elsevier.com/locate/bbagen

Biochemical characterization of tirabrutinib and other irreversible inhibitors of Bruton's tyrosine kinase reveals differences in on - and off - target inhibition

Albert Liclican, Loredana Serafini, Weimei Xing, Gregg Czerwieniec, Bart Steiner, Ting Wang, Katherine M. Brendza[1], Justin D. Lutz, Kathleen S. Keegan, Adrian S. Ray[2], Brian E. Schultz, Roman Sakowicz, Joy Y. Feng*

Gilead Sciences Inc, 333 Lakeside Drive, Foster City, CA 94404, United States of America

ARTICLE INFO

Keywords:
Bruton's tyrosine kinase
BTK inhibitor
Inactivation kinetics
Tirabrutinib
Ibrutinib

ABSTRACT

Background: Bruton's tyrosine kinase (BTK) is a key component of the B-cell receptor (BCR) pathway and a clinically validated target for small molecule inhibitors such as ibrutinib in the treatment of B-cell malignancies. Tirabrutinib (GS-4059/ONO-4059) is a selective, once daily, oral BTK inhibitor with clinical activity against many relapsed/refractory B-cell malignancies.

Methods: Covalent binding of tirabrutinib to BTK Cys-481 was assessed by LC-MSMS analysis of BTK using compound as a variable modification search parameter. Inhibition potency of tirabrutinib, ibrutinib, acalabrutinib, and spebrutinib against BTK and related kinases was studied in a dose-dependent manner either after a fixed incubation time (as used in conventional IC_{50} studies) or following a time course where inactivation kinetics were measured.

Results: Tirabrutinib irreversibly and covalently binds to BTK Cys-481. The inactivation efficiency k_{inact}/K_i was measured and used to calculate selectivity among different kinases for each of the four inhibitors studied. Tirabrutinib showed a k_{inact}/K_i value of $2.4 \pm 0.6 \times 10^4\ M^{-1}\ s^{-1}$ for BTK with selectivity against important off-targets.

Conclusions: For the BTK inhibitors tested in this study, analysis of the inactivation kinetics yielded a more accurate measurement of potency and selectivity than conventional single-time point inhibition measurements. Subtle but clear differences were identified between clinically tested BTK inhibitors which may translate into differentiated clinical efficacy and safety.

General significance: This is the first study that offers a detailed side-by-side comparison of four clinically-relevant BTK inhibitors with respect to their inactivation of BTK and related kinases.

1. Introduction

BTK is a member of the TEC family of cytoplasmic protein tyrosine kinases and a key component of the B-cell receptor (BCR) signaling pathway [1]. BCR signaling regulates cellular proliferation and activation, and promotes survival, differentiation, and clonal expansion of B cells [2]; however, aberrant BTK activation is a key oncogenic driver in a spectrum of B-cell malignancies [3,4]. In addition, BTK activity in innate immune effector cells transduces Fc receptor-mediated signaling, implicating its involvement in inflammatory diseases [5]. Targeting BTK for B-cell malignancies has been clinically validated by small molecule inhibitors (Fig. 1) [6–10]. The first generation irreversible BTK inhibitor, ibrutinib, has been a transformative therapy for patients with chronic lymphocytic leukemia (CLL)/small lymphocytic lymphoma (SLL), Waldenström's macroglobulinemia (WM), mantle cell lymphoma (MCL), and marginal zone lymphoma (MZL) [11,12]. In 2017, ibrutinib was approved for steroid-resistant chronic graft versus host disease (cGVHD) [13]. In recognition of the ibrutinib off-target activity against other kinases, second generation BTK inhibitors were designed for improved selectivity.

* Corresponding author.
E-mail address: joy.feng@gilead.com (J.Y. Feng).
[1] Currently at Nektar Therapeutics, 455 Mission Bay Boulevard South, San Francisco, CA 94158
[2] Currently at Morphic Therapeutic, 35 Gatehouse Drive, A2, Waltham, MA 02451

https://doi.org/10.1016/j.bbagen.2020.129531
Received 27 August 2019; Received in revised form 23 December 2019; Accepted 13 January 2020
Available online 15 January 2020

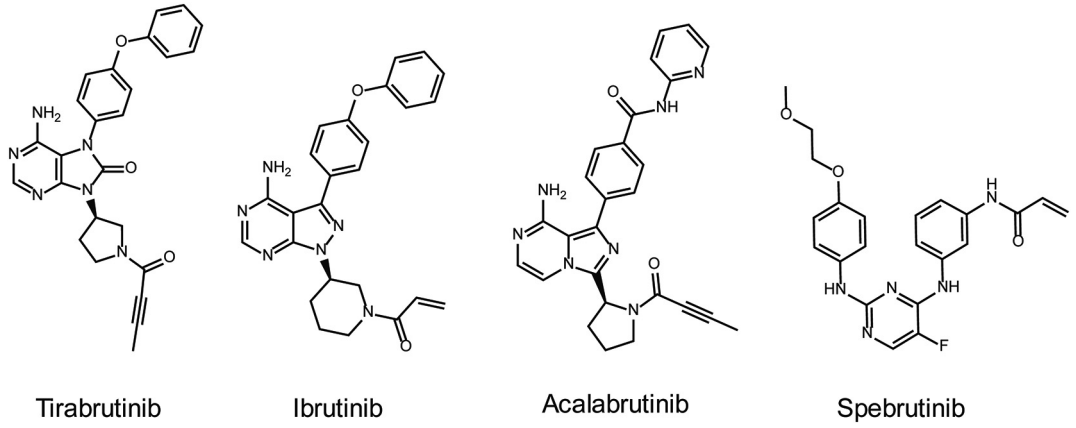

Fig. 1. Chemical structures of covalent BTK inhibitors tested in this study.

Ibrutinib showed sub-nanomolar biochemical activity against BTK [13] and covalent binding to BTK based on mass spectrometry, while its binding at Cys-481 residue was inferred from computer modeling of the BTK active site [14]. A mutation at Cys-481 (C481S) was later identified in ibrutinib-resistant patients and a ~500-fold decrease in potency was observed using recombinant mutant BTK [15]. In addition to BTK, ibrutinib also showed activity against at least nine other kinases that contain a cysteine homologous with Cys-481, including ITK, TEC, B lymphocyte kinase (BLK), and Janus kinase 3 (JAK3), as well as EGFR and human epidermal growth factor 2 (HER2) [11,13]. This broad activity may have therapeutic implications. Clinical observations of bleeding, rash, diarrhea, and atrial fibrillation in ibrutinib-treated patients [16,17] have been attributed to inhibition of TEC, EGFR, and other TEC family proteins besides BTK [18]. Tirabrutinib, acalabrutinib, and spebrutinib are designed to share the same mechanism of action as ibrutinib with improved specificity [19–21]; however, expected clinical safety improvement over ibrutinib has yet to be demonstrated [22].

Among many of the papers characterizing covalent BTK inhibitors, the enzyme inhibition of BTK and related kinases is typically quantified in terms of an IC_{50} value, the inhibitor concentration that causes a 50% decrease in enzyme activity. This is suitable for reversible inhibitors where the IC_{50} value is a measure of binding affinity under equilibrium conditions; however, the IC_{50} value is an inappropriate measurement for irreversible covalent inhibitors. An irreversible inhibitor is in effect infinitely potent, will titrate its enzyme target and yield an IC_{50} value dictated by the concentration of enzyme used in the inhibition assay. If an IC_{50} value for an irreversible inhibitor is higher than the enzyme concentration, it is an indication that the reaction of inhibitor with enzyme has not had sufficient time to go to completion [23]. Because of the ease and high-throughput adaptability of performing IC_{50} assays compared to more complex inactivation assays, IC_{50} values are frequently reported for potency and selectivity of irreversible covalent BTK inhibitors [13,19,21,24,25].

A more accurate assessment of the activity of irreversible inhibitors is achieved through characterization of the kinetics of enzyme inactivation rather than by a thermodynamic potency value. The binding of most irreversible inhibitors can be described by the mechanism in Scheme 1, in which there is a reversible, pre-equilibrium binding of inhibitor to enzyme characterized by the binding constant K_i, and an irreversible, covalent modification step described by the first-order rate constant k_{inact}. The ratio of k_{inact}/K_i, the inactivation efficiency, can be used to compare the inactivation kinetics of different irreversible, covalent inhibitors. Mathematically, the ratio k_{inact}/K_i has the form of a second-order rate constant, and is applicable when the concentration of inhibitor is below the K_i value for pre-binding of inhibitor to enzyme. The same methodology needs to be applied to study both the on-target inhibition of BTK and the potential off-target inhibition of related kinases that share an active site cysteine and are covalently inactivated.

$$E + I \underset{}{\overset{K_i}{\rightleftharpoons}} E\text{-}I \xrightarrow{k_{inact}} E\text{-}I^*$$

Scheme 1. Reaction scheme for irreversible inhibition.

Here we present our investigation of the mechanism of action for tirabrutinib, a selective, once daily, oral inhibitor of BTK with clinical activity against a number of relapsed/refractory B-cell malignancies [21,26]. The acyl alkyne reactive group of tirabrutinib was designed to specifically form a covalent bond with the Cys-481of the BTK active site, which was experimentally confirmed using mass spectrometry. Furthermore, BTK, EGFR and a set of TEC family kinases were studied for their inactivation by tirabrutinib, ibrutinib, acalabrutinib, and spebrutinib, and compound selectivity was calculated and compared. Tirabrutinib showed ~15-fold, 2.6-fold, and 2.7-fold higher selectivity for EGFR, ITK, and BMX, respectively, and 2.4-fold lower selectivity for TEC compared to ibrutinib.

2. Materials and methods

2.1. Materials

Full-length BTK containing an N-terminal His tag was expressed using a baculovirus expression system (Carna Biosciences, Chuo-ku, Kobe, Japan). In addition, full-length BTK containing an N-terminal GST tag was produced in-house. EGFR was purchased from BPS Biosciences (San Diego, CA); ITK, BMX, and TEC were purchased from Carna Biosciences. Tirabrutinib and other BTK inhibitors were synthesized at Gilead Sciences (Foster City, CA). Sulfonamido-oxine (Sox) chromophore peptide substrates for inactivation studies were purchased from AssayQuant Technologies (Marlboro, MA).

2.2. Methods

2.2.1. BTK expression and purification

The in-house full-length BTK containing an N-terminal GST tag was cloned into a pFastBac1 vector and the recombinant baculovirus was generated using Sf9 insect cells. For protein expression, the amplified baculovirus was used to infect Sf9 cells at 1.5×10^6 cells/mL, and the optimized virus amount was used for large-scale expression. Infected cells were grown at 27 °C, harvested 65 h post infection by centrifugation and stored at −80 °C. To purify the GST-BTK protein, 1 L cell pellet was suspended in 100 mL lysis buffer [25 mM Tris (pH 8.0), 300 mM NaCl, 0.5% (*v*/v) Triton X-100, and 1 mM DTT] supplemented with two tablets of Protease Inhibitor Cocktail (Roche Diagnostics, Risch-Rotkreuz, Switzerland). After the cells were lysed with a dounce

homogenizer, GST-BTK protein was purified from the clarified supernatant by glutathione-affinity chromatography, and eluted in loading buffer [25 mM Tris (pH 8.0), 200 mM NaCl, 0.05% (*v*/v) brij-35, and 1 mM DTT] supplemented with 20 mM reduced glutathione. The fractions from glutathione-affinity column were pooled, concentrated, and further purified by size exclusion chromatography (SEC) using a 24-mL Superose 6 column equilibrated with loading buffer. Fractions containing pure GST-BTK protein were concentrated and stored at −80 °C.

2.2.2. Determination of covalent binding

Protein labeling experiments were performed using BTK (Carna) at a final concentration of 2 μM in a buffer solution containing 10 mM HEPES, pH 7.5, 150 mM sodium chloride, 10 mM magnesium chloride, 2 mM Tris(2-carboxyethyl)phosphine (TCEP), and 1% glycerol. Inhibitors were added to a final concentration of 10 μM, with a final concentration of 1% DMSO in all samples. Four conditions were tested, each run in triplicate: BTK + tirabrutinib, BTK + staurosporine, BTK + ibrutinib, and BTK + DMSO control. After compound addition, samples were incubated overnight at 4 °C in a rotating shaker (1200 rpm). After an 18-h incubation, aliquots were collected from each condition for analysis and this time point was termed t = pre-chase. A chase step was then performed with the remaining sample by addition of ibrutinib into the BTK + tirabrutinib and BTK + staurosporine samples to a final concentration of 100 μM. An equivalent amount of DMSO was added to the BTK + ibrutinib and BTK + DMSO control samples to maintain the same volume. After incubating for 6 h at 4 °C, the remaining sample was collected at the final time point, termed t = post-chase. Aliquots taken at both time points were analyzed at the time of collection using mass spectrometry and enzyme activity assays.

Mass spectrometry analysis was performed on an Agilent 6210 Time of Flight Mass Spectrometer with an Agilent 1200 Rapid Resolution HPLC using Masshunter B.05 Acquisition software (Agilent, Santa Clara, CA). Samples were run on an Agilent Zorbax 300 Extend C18 rapid resolution column at 70 °C, using reverse phase chromatography with a gradient from 20% to 90% acetonitrile containing 0.1% formic acid. Data were processed using Agilent MassHunter Qualitative Analysis B.06, with a BioConfirm workflow allowing for protein deconvolution to obtain neutral mass values.

2.2.3. Covalent binding to BTK Cys-481

Samples were prepared as follows: 25 μg (2 μM) of in-house recombinant BTK protein was incubated in 50 mM ammonium bicarbonate and 10 μM tirabrutinib for 1 h at 37 °C. Samples were then reduced using 5 mM DTT at 55 °C for 45 min, followed by alkylation with 10 mM iodoacetamide at 25 °C for 1 h. Samples were then digested using a 50:1 ratio of GluC endoproteinase for 12 h at 37 °C, followed by addition of trypsin at a 50:1 ratio and another 4-h digestion at 37 °C to yield the expected peptide target of BTK with sequence YMANGCLLNYLR. Digested samples were then lyophilized and re-suspended in 3% acetonitrile, 0.1% formic acid and submitted for mass spectrometry analysis.

Mass spectrometry analysis was conducted as follows: Samples were injected using a ThermoFisher UltiMate 3000 RSLCnano System (San Jose, CA). Separation was performed using a ThermoFisher Scientific ES800 Easy Spray LC column (150 mm × 75 μm) at a flow rate of 300 nL/min on a 60-min gradient using 1% acetonitrile, 0.1% formic acid as solvent A and 90% acetonitrile, 0.1% formic acid as solvent B [3% B - 35% B (45 min), 35% B - 90% B (15 min), 90% B (5 min), re-equilibration (20 min)]. Mass spectrometry analysis was performed on a ThermoFisher Q-Exactive HF using a top 20 data dependent acquisition. Automatic gain control settings used 50 ms fill time and 3E6 ion counts for MS scans (60 K resolution) and 100 ms file times and 1E5 ion counts for MSMS scans (15 K resolution). Data were searched using Proteome Discoverer 2.2 against a Swissprot human database using variable chemical modification by tirabrutinib.

2.2.4. IC_{50} determination against BTK and other tyrosine kinases by tirabrutinib, ibrutinib, acalabrutinib, and spebrutinib in Z'-LYTE™ and LanthaScreen™ assays

The IC_{50} values of tirabrutinib, ibrutinib, acalabrutinib, and spebrutinib were first studied in a standard Z'-LYTE™ kinase or LanthaScreen™ binding assay against BTK and other TEC family kinases at Life Technologies/ThermoFisher Scientific (Waltham, MA). Various enzyme concentrations were used in each biochemical assays. The concentration of each enzyme was as follows: 0.26 nM BLK, 6.2 nM BMX, 3.1 nM BTK, 8.3 nM EGFR, 17.5 nM ERBB2, 16.2 nM ERBB4, 30.0 nM ITK, 2.7 nM JAK3, 8.1 nM TXK, and 1 nM TEC. The reactions were carried out at room temperature for 1 h. Detailed assay conditions can be found in the Supplementary Data.

2.2.5. BTK enzyme activity and IC_{50} evaluation

BTK activity was quantified by determining phosphorylation of a fluorescein-labeled substrate using a LanthaScreen™ Assay Kit (Life Technologies/ThermoFisher Scientific, Waltham, MA). The final reaction mixture contained kinase Buffer A [50 mM HEPES (pH 7.5), 10 mM $MgCl_2$, 0.01% brij-35, 1 mM EGTA, and 0.5 mg/mL BSA], 200–300 pM of BTK, 0.2 μM of fluorescein-Poly GT substrate, and 180 μM of ATP (2× K_m). All pre-incubations and reactions were carried out in black, 96-well nonbinding surface (NBS™) assay plates (Corning, Corning, NY) at room temperature. To evaluate the enzyme activity in the samples used in the mass spectrometry analysis, an aliquot of each of the samples was diluted to 300 pM BTK and 1.5 nM inhibitor in kinase reaction Buffer A. For IC_{50} determinations, compound dilutions were prepared using an HP D300 liquid dispenser (Hewlett-Packard, Palo Alto, CA) and the final DMSO concentration in the reactions was kept at 1%. After a 30-min pre-incubation of inhibitors and BTK in Buffer A, the kinase reaction was initiated by addition of an equal volume of 2× fluorescein-Poly GT substrate and ATP in Buffer A to reach a final 100 μL reaction mixture containing 200 pM BTK.

The kinase reaction was allowed to proceed for 30 min and was terminated with 100 μL of 2× EDTA/LanthaScreen™ Tb-PY20 antibody mixture in Life Technologies' TR-FRET Dilution Buffer to reach final concentrations of 10 mM EDTA and 2 nM antibody. Reactions were then incubated for at least 90 min at room temperature before fluorescence intensity (λ ex 332 nm/λ em 486/515 nm) was read on a TECAN Infinite M1000 Pro Multimode reader (Tecan Group Ltd., Männedorf, Switzerland). The ratio of fluorescence at 515 nm to that at 486 nm was the measure of product formation. The TR-FRET ratio was plotted against the inhibitor concentration and normalized to enzyme/no enzyme controls. IC_{50} values were calculated with a four-parameter logistic fit using GraphPad Prism (Version 6, La Jolla, CA).

2.2.6. Determination of inactivation kinetics for BTK

The rate of enzyme inactivation was studied as a function of inhibitor concentration using a Sox-based fluorescence assay that allows real-time measurement of enzyme activity [27]. In this assay, kinase activity is measured by an increase in fluorescence as a result of phosphorylation of a Sox-labeled substrate (AssayQuant Technologies, Marlboro, MA). Briefly, a Master Mix containing 1.3× Sox-labeled substrate, ATP, and DTT was prepared in reaction Buffer B [20 mM Tris-HCl (pH 7.5), 5 mM β-glycerophosphate, 1 mM EGTA, 5 mM $MgCl_2$, and 5% glycerol]. 75 μL of the Master Mix was added to the assay plate containing 1 μL compound solution in DMSO. Reactions were initiated with the addition of 25 μL of 4× in-house recombinant BTK protein in reaction Buffer B, except for the no-enzyme control in which only reaction Buffer B was used. The final assay mixtures contained 5 nM BTK, 10 μM Sox-labeled substrate AQT0101 (AQT0104 for ibrutinib) (AssayQuant), 300 μM ATP (2× K_m), and 200 μM DTT in reaction Buffer B. Fluorescence intensity readings (λ ex 360 nm/λ em 485 nm) were collected every 30 s for 4 h at room temperature using a TECAN Infinite

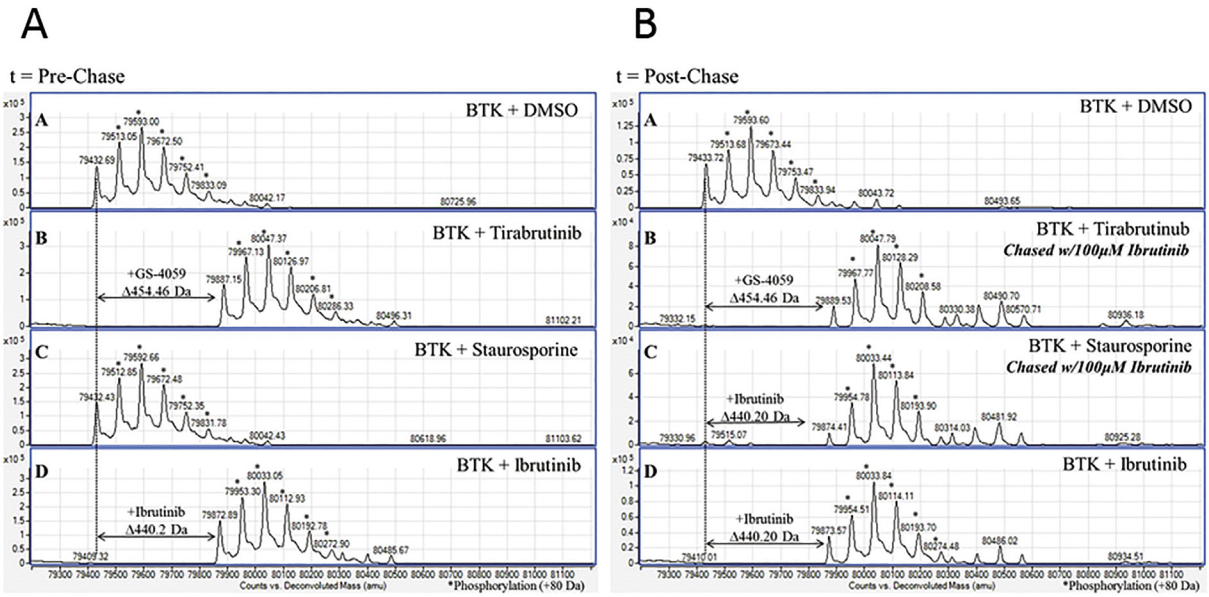

Fig. 2. Mass spectrometry demonstrating tirabrutinib covalently bound to BTK. (A) The mass shift of BTK upon binding of tirabrutinib. The reversible noncovalent inhibitor staurosporine and the irreversible covalent inhibitor ibrutinib were used as controls. (B) The mass shift of BTK upon binding of tirabrutinib after 6-h incubation with 100 mM ibrutinib.

M1000 Pro plate reader.

At the conclusion of each assay, background signal from no-enzyme controls was subtracted from all progress curves. Background subtracted progress curves were fit according to an ascending single-exponential equation to yield k_{obs} values (Eq. (1))

$$[P] = (v_0/k_{obs}) \times (1 - e^{-k_{obs} \times t}) \quad (1)$$

where $[P]$ is product concentration, v_o is the initial velocity in the presence of an inhibitor, k_{obs} is the rate constant, and t is time. The k_{obs} values at each compound concentration were determined using GraphPad Prism. Plots of k_{obs} versus inhibitor concentration, [inhibitor], were then fit to a hyperbolic equation to generate values for k_{inact} and K_i (Eq. (2)),

$$k_{obs} = k_{\text{inact}} \times [I]/([I] + K_i/(1 + [S]/K_m)) \quad (2)$$

where $[I]$ is the inhibitor concentration, $[S]$ is the substrate concentration, and K_m is the substrate concentration that results in half-maximal velocity for the enzyme reaction. In cases where individual values for k_{inact} and K_i could not be determined, the ratio of k_{inact}/K_i were reported. This ratio is the slope determined by linear fitting. Data from independent (n) experiments were averaged to yield values for k_{inact}/K_i.

2.2.7. Determination of inactivation kinetics for EGFR, BMX, ITK, and TEC

Enzymatic inhibition by tirabrutinib, ibrutinib, acalabrutinib, and spebrutinib were tested against EGFR and the TEC family kinases BMX, ITK, and TEC. Inactivation kinetics for the inhibitors were studied in a similar manner as previously described for BTK: EGFR at 2.5 nM with 70 mM ATP ($2\times K_m$), BMX at 1.25 nM with 100 mM ATP ($2\times K_m$), ITK at 5 nM with 50 mM ATP ($2\times K_m$), and TEC at 2.5 nM with 80 mM ATP ($2\times K_m$). The Sox substrates used were AQT0001 for EGFR, AQT0025 for BMX and ITK, and AQT0102 for TEC. Selectivity is defined as the ratio of the kinetic parameter k_{inact}/K_i for compound binding to BTK to k_{inact}/K_i for compound binding to EGFR, ITK, BMX, or TEC.

3. Results

3.1. Mass spectrometry demonstrated covalent and irreversible binding of tirabrutinib to BTK Cys-481

To determine if binding of tirabrutinib is covalent, the intact mass of BTK was measured for each sample at two different time points: (1) an 18-h incubation at 4 °C (t = pre-chase), and (2) an 18-h incubation at 4 °C followed by another 6-h incubation in the presence of 100 μM ibrutinib (t = post-chase). The deconvoluted mass spectra for representative samples at each time point are shown in Fig. 2. For the pre-chase samples, covalent adducts were visible for the BTK + tirabrutinib (+454 Da) and BTK + ibrutinib (+440 Da) treatments, with the additional mass matching the compound molecular weight within 1 Da (Fig. 2A). The BTK + staurosporine samples did not show a mass shift, consistent with the reversible inhibition mechanism of staurosporine [28]. After the 6-h chase with 100 μM ibrutinib, the BTK + staurosporine sample showed a mass shift of 440 Da, corresponding to the molecular weight of ibrutinib, indicating that the added ibrutinib displaced staurosporine and was covalently bound to BTK during post-chase (Fig. 2B). In contrast, the BTK + tirabrutinib samples continued to show a mass shift of 454 Da, corresponding to the molecular weight of tirabrutinib, instead of a mass shift of 440 Da as seen in the staurosporine post-chase sample. The inability of ibrutinib to displace tirabrutinib from its binding site on BTK indicated that tirabrutinib remained covalently bound to BTK even after incubating for 6 h with a high concentration of a competing inhibitor. Binding of tirabrutinib to Cys-481 was confirmed with BTK digested with trypsin and GluC endoproteinases followed by LC-MSMS. MS spectra with the exact mass corresponding to the mass of Cys-481- bound peptide YMANGCLLNYLR were obtained. MSMS spectra of the peptide were matched to theoretical b and y-ions for the peptide to confirm identity (Fig. S1). Mass spectra of the fragmentation of the bound peptide unambiguously identified the binding of tirabrutinib to active site Cys-481.

BTK activity of the mass spectrometry samples was verified at both t = pre-chase and t = post-chase time points as shown in Fig. S2. The samples were diluted 6667-fold from 2 μM BTK to 0.3 nM to ensure that the enzymatic activity was in the linear range for kinetic studies. As a result, the final concentration of staurosporine in the BTK + staurosporine sample was 1.5 nM, which was below the IC_{50}

Table 1
Inhibition of kinases by tirabrutinib using Z'-LYTE™ kinase assay.

Kinases[a]	Tirabrutinib		Ibrutinib		Acalabrutinib		Spebrutinib	
	IC_{50} (nM)	Selectivity[b]	IC_{50} (nM)	Selectivity	IC_{50} (nM)	Selectivity	IC_{50} (nM)	Selectivity
BTK	6.8	1.0	0.47	1.0	2.5	1.0	9.2	1
BLK	300	44	0.17	0.36	1020	410	400	43
BMX	6	0.88	0.86	1.8	36	14	5.5	0.60
EGFR	3020	440	3.8	8.1	7510	3000	> 20,000	> 2170
ERBB2	7313	1080	8.6	18	616	246	3500	380
ERBB4	770	113	2.0	4.3	12	4.8	220	24
ITK	> 20,000	> 2940	55	117	> 20,000	> 8000	1050	110
JAK3	5515	810	18	38	> 20,000	> 8000	36	3.9
TXK	92	14	1.9	4.0	170	68	29	3.2
TEC[c]	48	7.1	3.2	6.8	37	15	8.4	0.91

[a] BTK – Bruton's tyrosine kinase; BLK - B lymphocyte kinase; BMX – bone marrow expressed kinase; EGFR - epidermal growth factor receptor; ERBB-2 –human epidermal growth factor 2 receptor; ERBB4 - human epidermal growth factor 4 receptor; ITK - inducible T cell kinase, JAK – janus kinase; TXK – tyrosine protein kinase; and TEC - tyrosine kinase expressed in hepatocellular carcinoma. IC_{50} values were averages from 2 to 4 independent measurements.
[b] Selectivity = $(IC_{50})_{kinase}$: $(IC_{50})_{BTK}$.
[c] Inhibition of TEC was determined using LanthaScreen™ binding assay at Life Technologies/ThermoFisher Scientific.

concentration of 17 nM; therefore, a parallel sample containing freshly added 10 μM of staurosporine was added as a control. At the t = pre-chase time point, inhibition of BTK + tirabrutinib, BTK + staurosporine, BTK + staurosporine + additional 10 μM staurosporine, and BTK + ibrutinib was observed. As expected, the diluted solution of BTK + staurosporine showed 90% enzyme activity remaining while the sample treated with additional 10 μM staurosporine showed < 10% enzyme activity. At t = post-chase, all samples except the DMSO control showed inhibition of BTK activity as the result of ibrutinib addition.

3.2. IC_{50} determination against BTK and other tyrosine kinases by tirabrutinib, ibrutinib, acalabrutinib, and spebrutinib and time-dependence of IC_{50} values

The IC_{50} values of tirabrutinib, ibrutinib, acalabrutinib, and spebrutinib were first measured in a standard Z'-LYTE™ kinase or LanthaScreen™ binding assay against BTK and other TEC family kinases after 1-h pre-incubation with the enzymes (Table 1). In addition, a highly sensitive IC_{50} assay was developed in-house using a LanthaScreen™ endpoint assay which offered a sensitive method to test at enzyme concentrations as low as 0.2 nM BTK. IC_{50} values for tirabrutinib and other BTK inhibitors were determined after a 30-min pre-incubation of BTK with the inhibitors (Table 2). Ibrutinib showed an IC_{50} value of 0.46 ± 0.13 nM while the IC_{50} values for tirabrutinib, acalabrutinib, and spebrutinib were 7.0 ± 3.4, 3.0 ± 0.8, and 1.6 ± 0.7, and 3.0 ± 0.8 nM, respectively. A reversible BTK inhibitor, staurosporine, showed an IC_{50} value of 72 ± 17 nM. A set of representative IC_{50} curves is shown in Fig. S3 and summarized in Table 2. These observed IC_{50} values were consistent with published values [14,18,20,29,30].

Table 2
IC_{50} for BTK inhibitors measured in a LanthaScreen™ assay.

Inhibitor class	Compound	Alias	IC_{50} (nM)[a]
Covalent	Tirabrutinib	GS-4059/ONO-4059	7.0 ± 3.4 (n = 6)
	Ibrutinib	–	0.46 ± 0.13 (n = 5)
	Acalabrutinib	ACP-196	3.0 ± 0.8 (n = 5)
	Spebrutinib	CC-292	1.6 ± 0.7 (n = 5)
Reversible	Staurosporine	–	72 ± 17 (n = 3)

[a] The IC_{50} values were measured after a 30-min pre-incubation of 0.2 nM BTK with inhibitor. Data are in general agreement with published works: 2.2 nM for tirabrutinib [20], 0.5 nM for ibrutinib [14], 3.0 nM for acalabrutinib [18], and 90–210 nM for staurosporine [29,30]. The IC_{50} values are the average ± standard deviation of ≥3 independent experiments.

The IC_{50} values measured at 0.5, 1, 2, 3, and 4 h were extracted from the BTK inactivation kinetic studies mentioned above. As illustrated in Fig. 3E, all four BTK inhibitors showed decreased IC_{50} values as a function of time.

3.3. Kinetic parameters for inactivation of BTK and other kinases by covalent BTK inhibitors

The rate of enzyme inactivation was studied as a function of inhibitor concentration using a Sox-based fluorescence assay. As shown in Fig. 3A-D, the progress curves observed are typical of a slow-binding inhibitor when enzyme is added to initiate the reaction. The uninhibited enzyme reaction displayed a linear progress curve while the presence of the slow-binding inhibitors yielded progress curves with an exponential shape due to the slow onset of inhibition for such compounds. The progress curves were fitted with an equation for irreversible, slow-binding inhibitors (Eq. 1) to obtain rate constants, k_{obs}, at each inhibitor concentration. Plots of k_{obs} versus [inhibitor] were then fit to a hyperbolic equation (Eq. 2) as shown in Fig. S4. The exact values of k_{inact} and K_i could not be obtained due to two reasons: (1) the apparent high K_i values of the inhibitors; (2) the assay signal dropped below the level of detection at high inhibitor concentrations. Instead, the ratio of k_{inact}/K_i, a second-order rate determined by the slope using linear analysis, is used to describe the inactivation kinetics of the compound. The contribution of non-covalent binding to the inactivation kinetics could be probed by using a construct such as the C481S mutant of BTK [15], which should not form covalent adducts with the tested inhibitors, but this measurement is not necessary for a meaningful comparison of inactivation kinetics and was not pursued.

As summarized in Table 3, tirabrutinib efficiently inactivated BTK with a k_{inact}/K_i value of 2.4 ± 0.6 × 10^4 M^{-1} s^{-1}, similar to that of acalabrutinib (3.0 ± 0.9 × 10^4 M^{-1} s^{-1}) and spebrutinib (3.7 ± 0.1 × 10^4 M^{-1} s^{-1}), but > 10-fold lower than that of ibrutinib. The k_{inact}/K_i value for spebrutinib was consistent with the value reported in the literature (7.69 × 10^4 M^{-1} s^{-1}), using the same methodology [20]. The k_{inact}/K_i values were also determined for EGFR and the TEC family kinases BMX, ITK, and TEC. The k_{inact}/K_i values for ibrutinib were significantly higher compared to the other BTK inhibitors, as shown in Fig. S5 and Table 3, indicating it is a very potent inhibitor of BTK, EGFR, and other TEC family kinases including BMX, ITK, and TEC.

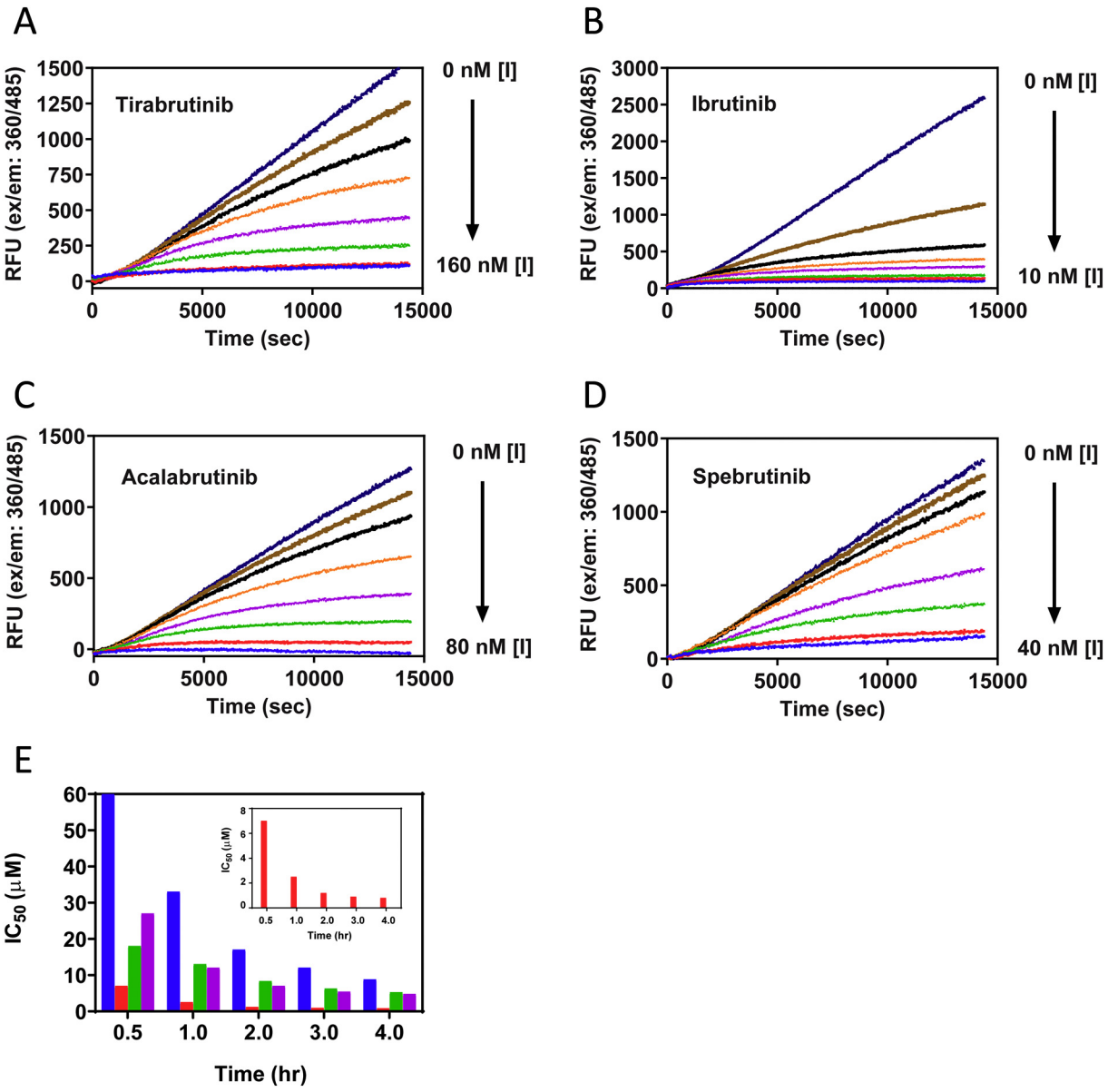

Fig. 3. BTK product formation progress curves (A-D) and time-dependence of IC_{50} values (E). In the presence of increasing concentrations of tirabrutinib (A), ibrutinib (B), acalabrutinib (C), and spebrutinib (D), the production of BTK phosphorylated peptide slows down as time progresses. Concentrations to the right of curves indicate the range of compound concentrations and a series of 2-fold dilutions were applied. (E) Time-dependence of IC_{50} values for tirabrutinib (blue), ibrutinib (red), acalabrutinib (green), and spebrutinib (purple). Inset graph: magnified view of IC_{50} values for ibrutinib (red).

Table 3
Kinetic parameters for inactivation of tirabrutinib and analogs for BTK and related kinases.

Kinases	Tirabrutinib		Ibrutinib		Acalabrutinib		Spebrutinib	
	k_{inact}/K_i (M^{-1} s^{-1})[a]	Selectivity[b]	k_{inact}/K_i (M^{-1} s^{-1})	Selectivity	k_{inact}/K_i (M^{-1} s^{-1})	Selectivity	k_{inact}/K_i (M^{-1} s^{-1})	Selectivity
BTK	2.4×10^4	1	1.0×10^6	1	3.0×10^4	1	3.7×10^4	1
BMX	3.6×10^4	0.67	3.9×10^6	0.25	1.9×10^4	16	1.6×10^4	2.3
EGFR	68	353	4.1×10^4	24	24	1250	80	463
ITK	26	923	2.8×10^3	357	7.0	4286	625	59
TEC	1.1×10^4	2.3	1.8×10^5	5.6	1.5×10^4	2.0	1.6×10^5	0.2

[a] The k_{inact}/K_i values are the average ± standard deviation of ≥3 independent experiments.
[b] Selectivity = $(k_{inact}/K_i)_{kinase}$: $(k_{inact}/K_i)_{BTK}$.

3.4. Selectivity of BTK inhibitors for BTK over other related kinases based on IC_{50} values and k_{inact}/K_i

The selectivity of BTK inhibitors towards BTK was assessed over ten tyrosine kinases that contain a cysteine residue at a homologous position as Cys-481 in BTK using the IC_{50} values (Table 1). The selectivity is defined as Selectivity^{IC50}. In parallel, selectivity over the four kinases BMX, EGFR, ITK, and TEC, defined as Selectivity$^{kinact/Ki}$, was calculated and summarized in Table 3. Overall, these two methods offered similar rank orders of selectivity but Selectivity^{IC50} values tend to exaggerate selectivity relative to Selectivity$^{kinact/Ki}$ values. Based on Selectivity$^{kinact/Ki}$ values, tirabrutinib and ibrutinib showed the same order of selectivity with ITK > EGFR > TEC > BMX. Acalabrutinib showed a similar pattern of selectivity following ITK > EGFR > BMX > TEC, while spebrutinib showed a higher EGFR selectivity over ITK and followed the order of EGFR > ITK > BMX > TEC. However, tirabrutinib showed ~15-fold, 2.6-fold, and 2.7-fold higher selectivity for EGFR, ITK, and BMX, respectively, and 2.4-fold lower selectivity for TEC compared to ibrutinib.

4. Discussion

In this study, we used mass spectrometry to demonstrate that tirabrutinib covalently binds to BTK at the Cys-481 site. We then used detailed kinetic analysis to illustrate that tirabrutinib and three other clinically relevant BTK inhibitors inactivated BTK in a time-dependent manner. Our data showed that tirabrutinib is a potent and selective inhibitor of BTK over other related tyrosine kinases including TEC family members.

Proper characterization of covalent inhibitors can be challenging since the degree of inhibition is both influenced by the amount of enzyme and the duration of inhibitor treatment, two key factors overlooked by the conventional IC_{50} measurement. As a result, a very potent inhibitor such as ibrutinib could be underestimated for its potency against on-target kinase BTK and this could lead to underestimate of its selectivity over off-target kinases. For example, the reported BTK IC_{50} values of ibrutinib, acalabrutinib, and spebrutinib were 1.5, 5.1, and 2.3 nM in a biochemical assay [19], while the final concentration of BTK was 4 nM, suggesting that the lowest IC_{50} value that any inhibitor can possibly reach is ~2 nM, where half of the enzymes were inhibited. Therefore, the reported IC_{50} values of 1.5 and 2.3 nM can only indicate that the assay has “bottomed out” or reached its lower limit of detection, instead of implying the true potency of the inhibitors tested. Furthermore, when an irreversible inhibitor is tested against a panel of related kinases, each IC_{50} value can be highly arbitrary based on each assay condition, and this leads to less accurate selectivity assessment. Inactivation data yields a more accurate characterization of these irreversible, covalent inhibitors. Until this study, the only inactivation data reported has been for spebrutinib [20].

Kinase selectivity data have the potential to assist in understanding toxicity liabilities. Bleeding is a toxicity associated with ibrutinib observed in the clinic. Off-target inhibition of TEC is believed to contribute to platelet dysfunction [31]. However, a recent study by Bye et al. suggested that Src family kinases (SFKs) but not Tec family kinases are responsible for the dysfunctional platelet thrombus formation caused by ibrutinib therapy [32]. This is consistent with the relatively low TEC selectivity of tirabrutinib, ibrutinib, and acalabrutinib in our study: Selectivity^{IC50} values of 8.7, 6.8, and 15, and Selectivity$^{kinact/Ki}$ values of 2.3, 5.6, and 2.0 for tirabrutinib, ibrutinib, acalabrutinib, respectively. It was suggested that selectivity over Src family kinases contributes to the favorable platelet function profile of acalabrutinib over ibrutinib in non-Hodgkin lymphoma (NHL) patients [32]. An ongoing Phase III randomized clinical trial (NCT02477696) is in progress to compare acalabrutinib to ibrutinib in previously treated subjects with high risk CLL and may address some of these questions. Another common adverse event associated with ibrutinib is rash, often attributed to inhibition of EGFR [33]. This is consistent with the lack of ibrutinib selectivity against EGFR observed in our study: the calculated Selectivity^{IC50} values for tirabrutinib and acalabrutinib are 630 and 3000 compared to a value of 3.8 for ibrutinib; and the calculated Selectivity$^{kinact/Ki}$ of 353 and 1250 for tirabrutinib and acalabrutinib, respectively, compared to a value of 24 for ibrutinib. Whether this improved selectivity will be reflected in clinical trial results remains to be seen. Notably, when covalent inhibitors are assessed for their selectivity in vivo, the differences in protein half-life should also be taken into consideration. This is a limitation of our current study and can be addressed in future works. Further improvement of the selectivity profile of irreversible BTK inhibitors to treat B-cell malignancies remains an area of great interest.

In summary, our study showed that tirabrutinib binds to BTK at Cys-481 and is a covalent irreversible inhibitor. Measurement of the inactivation kinetics of tirabrutinib showed improved selectivity against potential off-target enzymes BMX, EGFR, and ITK compared to ibrutinib. Among the 2nd generation inhibitors tirabrutinib, acalabrutininb, and spebrutinib there are subtle differences in selectivity patterns against off-target kinases; however, whether this translates into improved clinical efficacy and safety remains to be seen.

Supplementary data to this article can be found online at https://doi.org/10.1016/j.bbagen.2020.129531.

Declaration of Competing Interest

All authors are current or former employees and shareholders of Gilead Sciences, Inc.

Acknowledgements

We thank Dr. Juliane Juergensmeier and Dr. Jen Cain for their valuable insights and comments in the preparation of this manuscript.

References

[1] Y. Aoki, K.J. Isselbacher, S. Pillai, Bruton tyrosine kinase is tyrosine phosphorylated and activated in pre-B lymphocytes and receptor-ligated B cells, Proc. Natl. Acad. Sci. U. S. A. 91 (1994) 10606–10609.
[2] R.C. Rickert, New insights into pre-BCR and BCR signalling with relevance to B cell malignancies, Natl. Rev. 13 (2013) 578–591.
[3] M. Buchner, M. Muschen, Targeting the B-cell receptor signaling pathway in B lymphoid malignancies [author manuscript], Curr. Opin. Hematol. 21 (2014) 1–9.
[4] R. Kuppers, Mechanisms of B-cell lymphoma pathogenesis, Nat. Rev. Cancer 5 (2005) 251–262.
[5] F. Nimmerjahn, J.V. Ravetch, Fcgamma receptors as regulators of immune responses, Natl. Rev. 8 (2008) 34–47.
[6] J.C. Byrd, J.R. Brown, S. O'Brien, J.C. Barrientos, N.E. Kay, N.M. Reddy, S. Coutre, C.S. Tam, S.P. Mulligan, U. Jaeger, S. Devereux, P.M. Barr, R.R. Furman, T.J. Kipps, F. Cymbalista, C. Pocock, P. Thornton, F. Caligaris-Cappio, T. Robak, J. Delgado, S.J. Schuster, M. Montillo, A. Schuh, S. de Vos, D. Gill, A. Bloor, C. Dearden, C. Moreno, J.J. Jones, A.D. Chu, M. Fardis, J. McGreivy, F. Clow, D.F. James, P. Hillmen, Ibrutinib versus Ofatumumab in previously treated chronic lymphoid Leukemia, N. Engl. J. Med. 371 (3) (2014) 213–223.
[7] J.C. Byrd, R.R. Furman, S.E. Coutre, I.W. Flinn, J.A. Burger, K.A. Blum, B. Grant, J.P. Sharman, M. Coleman, W.G. Wierda, J.A. Jones, W. Zhao, N.A. Heerema, A.J. Johnson, J. Sukbuntherng, B.Y. Chang, F. Clow, E. Hedrick, J.J. Buggy, D.F. James, S. O'Brien, Targeting BTK with ibrutinib in relapsed chronic lymphocytic leukemia, N. Engl. J. Med. 369 (2013) 32–42.
[8] L. Liu, J. Di Paolo, J. Barbosa, H. Rong, K. Reif, H. Wong, Antiarthritis effect of a novel Bruton's tyrosine kinase (BTK) inhibitor in rat collagen-induced arthritis and mechanism-based pharmacokinetic/pharmacodynamic modeling: relationships between inhibition of BTK phosphorylation and efficacy, J. Pharmacol. Exp. Ther. 338 (2011) 154–163.
[9] J. Wu, C. Liu, S.T. Tsui, D. Liu, Second-generation inhibitors of Bruton tyrosine kinase, J. Hematol. Oncol. 9 (2016) 1–7.
[10] M. Wang, S. Rule, P.L. Zinzani, A. Goy, O. Casasnovas, S.D. Smith, G. Damaj, J. Doorduijn, T. Lamy, F. Morschhauser, C. Panizo, B. Shah, A. Davies, R. Eek, J. Dupuis, E. Jacobsen, A.P. Kater, S. LeGouill, L. Oberic, T. Robak, T. Covey, R. Dua, A. Hamdy, X. Huang, R. Izumi, P. Patel, W. Rothbaum, J.G. Slatter, W. Jurczak, Acalabrutinib in relapsed or refractory mantle cell lymphoma (ACE-LY-004): a single-arm, multicentre, phase 2 trial, Lancet 391 (2017) 659–667.
[11] M.S. Davids, J.R. Brown, Ibrutinib: a first in class covalent ihibitor of Bruton's tyrosine kinase, Future Oncol. 10 (2014) 957–967.
[12] A. Noy, S. de Vos, C. Thieblemont, P. Martin, C.R. Flowers, F. Morschhauser,

G.P. Collins, S. Ma, M. Coleman, S. Peles, S. Smith, J.C. Barrientos, A. Smith, B. Munneke, I. Dimery, D.M. Beaupre, R. Chen, Targeting Bruton tyrosine kinase with ibrutinib in relapsed/refractory marginal zone lymphoma, Blood 129 (2017) 2224–2232.

[13] L.A. Honigberg, A.M. Smith, M. Sirisawad, E. Verner, D. Loury, B. Chang, S. Li, Z. Pan, D.H. Thamm, R.A. Miller, J.J. Buggy, The Bruton tyrosine kinase inhibitor PCI-32765 blocks B-cell activation and is efficacious in models of autoimmune disease and B-cell malignancy, PNAS 107 (2010) 13075–13080.

[14] Z. Pan, H. Scheerens, S.J. Li, B.E. Schultz, P.A. Sprengeler, L.C. Burrill, R.V. Mendonca, M.D. Sweeney, K.C. Scott, P.G. Grothaus, D.A. Jeffery, J.M. Spoerke, L.A. Honigberg, P.R. Young, S.A. Dalrymple, J.T. Palmer, Discovery of selective irreversible inhibitors for Bruton's tyrosine kinase, ChemMedChem 2 (2007) 58–61.

[15] J.A. Woyach, R.R. Furman, T.M. Liu, H.G. Ozer, M. Zapatka, A.S. Ruppert, L. Xue, D.H. Li, S.M. Steggerda, M. Versele, S.S. Dave, J. Zhang, A.S. Yilmaz, S.M. Jaglowski, K.A. Blum, A. Lozanski, G. Lozanski, D.F. James, J.C. Barrientos, P. Lichter, S. Stilgenbauer, J.J. Buggy, B.Y. Chang, A.J. Johnson, J.C. Byrd, Resistance mechanisms for the Bruton's tyrosine kinase inhibitor ibrutinib, N. Engl. J. Med. 370 (2014) 2286–2294.

[16] M.L. Wang, S. Rule, P. Martin, A. Goy, R. Auer, B.S. Kahl, W. Jurczak, R.H. Advani, J.E. Romaguera, M.E. Williams, J.C. Barrientos, E. Chmielowska, J. Radford, S. Stilgenbauer, M. Dreyling, W.W. Jedrzejczak, P. Johnson, S.E. Spurgeon, L. Li, L. Zhang, K. Newberry, Z. Ou, N. Cheng, B. Fang, J. McGreivy, F. Clow, J.J. Buggy, B.Y. Chang, D.M. Beaupre, L.A. Kunkel, K.A. Blum, Targeting BTK with ibrutinib in relapsed or refractory mantle-cell lymphoma, N. Engl. J. Med. 369 (2013) 507–516.

[17] J.R. Brown, J.C. Barrientos, P.M. Barr, I.W. Flinn, J.A. Burger, A. Tran, F. Clow, D.F. James, T. Graef, J.W. Friedberg, K. Rai, S. O'Brien, The Bruton tyrosine kinase inhibitor Ibrutinib with chemoimmunotherapy in patients with chronic lymphocytic Leukemia, Blood 125 (2015) 2915–2922.

[18] J. Wu, M. Zhang, D. Liu, Acalabrutinib (ACP-196): a selective second-generation BTK inhibitor, J. Hematol. Oncol. 9 (2016) 1–4.

[19] T. Barf, T. Covey, R. Izumi, B. van de Kar, M. Gulrajani, B. van Lith, M. van Hoek, E. de Zwart, D. Mittag, D. Demont, S. Verkaik, F. Krantz, P.G. Pearson, R. Ulrich, A. Kaptein, Acalabrutinib (ACP-196): a covalent Bruton tyrosine kinase inhibitor with a differentiated selectivity and in vivo potency profile, J. Pharmacol. Exp. Ther. 363 (2017) 240–252.

[20] E.K. Evans, R. Tester, S. Aslanian, R. Karp, M. Sheets, M.T. Labenski, S.R. Witowski, H. Lounsbury, P. Chaturvedi, H. Mazdiyasni, Z. Zhu, M. Nacht, M.I. Freed, R.C. Petter, A. Dubrovskiy, J. Singh, W.F. Westlin, Inhibition of Btk with CC-292 provides early pharmacodynamic assessment of activity in mice and humans, J. Pharmacol. Exp. Ther. 346 (2013) 219–228.

[21] H.S. Walter, S.A. Rule, M.J. Dyer, L. Karlin, C. Jones, B. Cazin, P. Quittet, N. Shah, C.V. Hutchinson, H. Honda, K. Duffy, J. Birkett, V. Jamieson, N. Courtenay-Luck, T. Yoshizawa, J. Sharpe, T. Ohno, S. Abe, A. Nishimura, G. Cartron, F. Morschhauser, C. Fegan, G. Salles, A phase 1 clinical trial of the selective BTK inhibitor ONO/GS-4059 in relapsed and refractory mature B-cell malignancies, Blood 127 (2016) 411–419.

[22] P. Kapoor, S.M. Ansell, Acalabrutinib in mantle cell lymphoma, Lancet 391 (10121) (2017) 633–634.

[23] R.A. Copeland, Chapter 10 - time-dependent inhibition, Enzymes: A Practical Introduction to Structure, Mechanism, and Data Analysis, 2000, pp. 318–349.

[24] J.C. Byrd, B. Harrington, S. O'Brien, J.A. Jones, A. Schuh, S. Devereux, J. Chaves, W.G. Wierda, F.T. Awan, J.R. Brown, P. Hillmen, D.M. Stephens, P. Ghia, J.C. Barrientos, J.M. Pagel, J. Woyach, D. Johnson, J. Huang, X. Wang, A. Kaptein, B.J. Lannutti, T. Covey, M. Fardis, J. McGreivy, A. Hamdy, W. Rothbaum, R. Izumi, T.G. Diacovo, A.J. Johnson, R.R. Furman, Acalabrutinib (ACP-196) in relapsed chronic lymphocytic Leukemia, N. Engl. J. Med. 374 (2016) 323–332.

[25] J.A. Di Paolo, T. Huang, M. Balazs, J. Barbosa, K.H. Barck, B.J. Bravo, R.A. Carano, J. Darrow, D.R. Davies, L.E. DeForge, L. Diehl, R. Ferrando, S.L. Gallion, A.M. Giannetti, P. Gribling, V. Hurez, S.G. Hymowitz, R. Jones, J.E. Kropf, W.P. Lee, P.M. Maciejewski, S.A. Mitchell, H. Rong, B.L. Staker, J.A. Whitney, S. Yeh, W.B. Young, C. Yu, J. Zhang, K. Reif, K.S. Currie, Specific Btk inhibition suppresses B cell- and myeloid cell-mediated arthritis, Nat. Chem. Biol. 7 (2011) 41–50.

[26] T. Yasuhiro, T. Yoshizawa, H. Daub, C. Weber, M. Narita, K. Kawabata, ONOWG307, a novel, potent and selective inhibitor of Bruton's tyrosine kinase (Btk), results in sustained inhibition of the ERK, AKT and PKD signaling pathways [Abstract 2021], American Association for Cancer Research (AACR), 2012 Chicago, IL.

[27] M.D. Shults, D. Carrico-Moniz, B. Imperiali, Optimal Sox-based fluorescent chemosensor design for serine/threonine protein kinases, Anal. Biochem. 352 (2006) 198–207.

[28] H. Nakano, S. Omura, Chemical biology of natural indolocarbazole products: 30 years since the discovery of staurosporine, J. Antibiot. (Tokyo) 62 (2009) 17–26.

[29] M.W. Karaman, S. Herrgard, D.K. Treiber, P. Gallant, C.E. Atteridge, B.T. Campbell, K.W. Chan, P. Ciceri, M.I. Davis, P.T. Edeen, R. Faraoni, M. Floyd, J.P. Hunt, D.J. Lockhart, Z.V. Milanov, M.J. Morrison, G. Pallares, H.K. Patel, S. Pritchard, L.M. Wodicka, P.P. Zarrinkar, A quantitative analysis of kinase inhibitor selectivity, Nat. Biotechnol. 26 (2008) 127–132.

[30] M. Dinh, D. Grunberger, H. Ho, S.Y. Tsing, D. Shaw, S. Lee, J. Barnett, R.J. Hill, D.C. Swinney, J.M. Bradshaw, Activation mechanism and steady state kinetics of Bruton's tyrosine kinase, J. Biol. Chem. 282 (2007) 8768–8776.

[31] J.J. Shatzel, S.R. Olson, D.L. Tao, O.J.T. McCarty, A.V. Danilov, T.G. DeLoughery, Ibrutinib-associated bleeding: pathogenesis, management and risk reduction strategies, J. Thromb. Haemost. 15 (2017) 835–847.

[32] A.P. Bye, A.J. Unsworth, M.J. Desborough, C.A.T. Hildyard, N. Appleby, D. Bruce, N. Kriek, S.H. Nock, T. Sage, C.E. Hughes, J.M. Gibbins, Severe platelet dysfunction in NHL patients receiving ibrutinib is absent in patients receiving acalabrutinib, Blood Adv. 1 (2017) 2610–2623.

[33] C. Robert, J.C. Soria, A. Spatz, A. Le Cesne, D. Malka, P. Pautier, J. Wechsler, C. Lhomme, B. Escudier, V. Boige, J.P. Armand, T. Le Chevalier, Cutaneous side-effects of kinase inhibitors and blocking antibodies, Lancet Oncol. 6 (2005) 491–500.